NEOPLASIA
www.neoplasia.com

Volume 11 Number 7 July 2009 pp. 637–650 637

Gemcitabine-Based Chemogene Therapy for Pancreatic Cancer Using Ad-dCK::UMK GDEPT and TS/RR siRNA Strategies[1]

Soukaina Réjiba, Christelle Bigand, Céline Parmentier and Amor Hajri

Digestive Cancer Research Institute, Tumor Biology & Gene Therapy Department, IRCAD – INSERM Unit 701, F67091-Strasbourg, France

Abstract

Gemcitabine is a first-line agent for advanced pancreatic cancer therapy. However, its efficacy is often limited by its poor intracellular metabolism and chemoresistance. To exert its antitumor activity, gemcitabine requires to be converted to its active triphosphate form. Thus, our aim was to improve gemcitabine activation using gene-directed enzyme prodrug therapy based on gemcitabine association with the deoxycytidine kinase::uridine monophosphate kinase fusion gene (dCK::UMK) and small interference RNA directed against ribonucleotide reductase (RRM2) and thymidylate synthase (TS). *In vitro*, cytotoxicity was assessed by 3-[4,5-dimethylthiazol-2-yl]-3,5-diphenyl tetrazolium bromide and [^{3}H]thymidine assays. Apoptosis-related gene expression and activity were analyzed by reverse transcription–polymerase chain reaction, Western blot, and ELISA. For *in vivo* studies, the treatment efficacy was evaluated on subcutaneous and orthotopic pancreatic tumor models. Our data indicated that cell exposure to gemcitabine induced a down-regulation of dCK expression and up-regulation of TS and RR expression in Panc1-resistant cells when compared with BxPc3- and HA-hpc2–sensitive cells. The combination of TS/RRM2 small interference RNA with Ad-dCK::UMK induced a 40-fold decrease of gemcitabine IC_{50} in Panc1 cells. This strong sensitization was associated to apoptosis induction with a remarkable increase in TRAIL expression and a diminution of gemcitabine-induced nuclear factor-κB activity. *In vivo*, the gemcitabine-based tritherapy strongly reduced tumor volumes and significantly prolonged mice survival. Moreover, we observed an obvious increase of apoptosis and decrease of cell proliferation in tumors receiving the tritherapy regimens. Together, these findings suggest that simultaneous TS/RRM2-gene silencing and dCK::UMK gene overexpression markedly improved gemcitabine's therapeutic activity. Clearly, this combined strategy warrants further investigation.

Neoplasia (2009) 11, 637–650

Introduction

Pancreatic adenocarcinoma is one of the most deadly forms of cancer. With a 5-year survival rate of only 3% and a median survival of less than 6 months, diagnosis of pancreatic adenocarcinoma is fatal for patients. The tendency is for highly aggressive locoregional invasion making curative surgery impossible [1]. Conventional chemotherapy and radiotherapy, alone or in combination, have limited effect on the overall survival of patients with pancreatic cancer [2]. Recently, gemcitabine (2′,2′-difluorodeoxycytidine) has emerged as the first-line treatment of locally advanced and metastatic pancreatic cancers [3–5]. It is the treatment of choice as a single agent or in combination with other cytotoxic agents for solid tumors including ovarian, non–small cell lung, and pancreatic cancers [6–8].

The antitumor activity of gemcitabine is exerted by its phosphorylated metabolites. After translocation across the cellular membrane by nucleoside transporters [9], gemcitabine is phosphorylated to its monophosphate (dFdCMP) form by the deoxycytidine kinase (dCK) in a rate-limiting step. Then, other nucleoside kinases further phosphorylate dFdCMP to its two active diphosphate and triphosphate (dFdCTP) forms [10–12]. The dFdCTP competes with the natural deoxycytidine-triphosphate analog for incorporation in DNA and RNA [13,14], causing

Address all correspondence to: Soukaina Réjiba, 8 rue d'Ensisheim - 67100, Strasbourg, France. E-mail: srejiba@yahoo.fr

[1]This work was supported by "association pour la recherche sur le cancer" and "club français du pancréas."

Received 2 January 2009; Revised 26 March 2009; Accepted 20 April 2009

DOI 10.1593/neo.81686

masked chain termination [11,12], and inhibits CTP synthase. This effect blocks the *de novo* DNA synthesis pathway.

Unfortunately, despite its promising activity against cancer cells, response rates to gemcitabine in pancreatic cancers remain low, with less than 20% objective response in clinical cases [3–5]. After injection, gemcitabine is often confronted with poor phosphorylation to its active triphosphate metabolite, rapid deactivation, and emergence of chemoresistance. Insufficient intracellular concentration of dFdCTP because of inefficient cellular uptake, reduced levels of gemcitabine activation, or increased drug degradation can be cited among the numerous mechanisms of resistance acquired during or after gemcitabine treatment [15].

In the present study, we hypothesized that altered expression/activity of enzymes directly involved in gemcitabine metabolism constitutes an important form of chemoresistance. Deficiency in dCK activity has been considered as one of the main mechanisms responsible for the development of resistance to gemcitabine. Several authors have described a relationship between dCK activity and sensitivity to gemcitabine in cells with acquired resistance to gemcitabine [16–18]. In this context, gene therapy may enhance gemcitabine metabolism and, consequently, improve tumor cell responsiveness to this prodrug. Some studies emphasizing the first limiting step of gemcitabine phosphorylation by overexpression of dCK in tumor cells deficient in this enzyme have shown restoration of the sensitivity to gemcitabine [15,19,20]. Moreover, gemcitabine phosphorylation can be improved by uridine monophosphate kinase (UMK) overexpression. UMK phosphorylates CMP, UMP, and dCMP to their respective diphosphate forms [21], and UMK has been shown to play an important role in the activation of deoxycytidine analogs [22,23]. A fusion gene combining dCK with UMK was shown to be efficient in sensitizing hamster pancreatic cancer cells to gemcitabine treatment [24].

In parallel, several data support the hypothesis that gemcitabine resistance may also be dependent on ribonucleotide reductase (RR) and thymidylate synthase (TS) overexpression [25,26]. Thus, small interference RNA (siRNA) targeting TS and RR can be of great interest for specific TS and RR gene silencing. Recently, it was demonstrated that RRM2 siRNA targeting the subunit responsible for RR activity enhanced gemcitabine-induced cytotoxicity both *in vitro* and *in vivo* [26,27]. Obviously, the concomitant inhibition of TS and RR expression would thus promote sensitization to gemcitabine in different ways, including the reversal of dCK activity inhibition, and a competitively higher incorporation of dFdCTP into DNA.

The purpose of the present study was to improve gemcitabine efficacy by increasing gemcitabine anabolism, acting especially on the dCK, TS, and RR enzymes. We investigated potential changes in dCK, TS, and RR expression and examined whether gemcitabine therapy improvement can be accomplished by an anticancer gene-directed enzyme prodrug therapy (GDEPT) strategy that provides enhanced dCK::UMK fusion gene expression associated with specific TS and RR gene silencing. To this end, an adenovirus expressing the dCK::UMK fusion protein and siRNA directed against TS and RRM2 were used to favor conversion of gemcitabine into its toxic phosphorylated metabolite and circumvent existing chemoresistance. The effect of gemcitabine combination with Ad-dCK::UMK and TS/RRM2 siRNA was assessed on cell survival and apoptosis both *in vitro* and *in vivo* on subcutaneous and orthotopic pancreatic tumor models.

The current study demonstrated that simultaneous dCK::UMK overexpression and TS/RRM2 gene silencing significantly improved the antitumor activity of gemcitabine. Furthermore, apoptosis seems to be a major mechanism of the potent induced tumor cell death.

Materials and Methods

Cell Cultures

Human pancreatic cell lines BxPc3 and Panc1 from ATCC (LGC Promochem, France), HA-hpc2 (developed in our laboratory from human pancreatic metastasis), and human embryonic kidney AD293 cell line (Stratagene, France) were maintained at 37°C in a humid atmosphere with 5% CO_2. Panc1, HA-hpc2, and AD293 cells were grown in Dulbecco's modified Eagle medium–Glutamax medium, whereas BxPc3 cells were grown in RPMI 1640–Glutamax. Media were supplemented with 10% heat-inactivated fetal calf serum, penicillin (100 U/ml), and streptomycin (100 μg/ml). All reagents were purchased from Invitrogen (Cergy Pontoise, France).

Vector Constructs and Adenovirus Production

For the fusion gene dCK::UMK, the self-cleaving FMDV 2A peptide was inserted between dCK and UMK (Cayla, Toulouse, France). The cDNA corresponding to human dCK and dCK::UMK were recovered by polymerase chain reaction (PCR) from pVIVOTKSh-DCK and pVIVOTKSh-DU plasmids (Cayla), respectively, using specific primers. The PCR fragments were converted to blunt ends, and their 5′ ends were phosphorylated with T4 polynucleotide kinase (New England Biolabs, Ozyme, Saint Quentin en Yvelines, France). Each insert was then ligated into the *Eco*RV site of pShuttle-CMV using T4 ligase (New England Biolabs). Thereafter, the two recombinant plasmids were grown in *Escherichia coli* strain DH5α and were used to obtain the corresponding recombinant adenoviruses according to Stratagene instructions. Briefly, the resulting clones were linearized with *Pme*I and recombined with pAdEasy-1 in BJ5183-AD-1 bacteria. Purified recombinant plasmids were linearized by *Pac*I restriction enzyme and subsequently transfected into the adenovirus *E1* gene–producing AD293 cells to create adenoviruses. Recombinant viruses were propagated in AD293 cells, purified by CsCl step gradient ultracentrifugation, and tittered by standard methods [28,29].

siRNA Transfection

Tumor cells (70% of confluence) were transfected with 100 nM of TS and/or RRM2 siRNA using Lipofectamine 2000 (Invitrogen) according to the manufacturer's protocol.

Expression Analysis

Analyses of gene expression were all performed after 48 hours of gemcitabine treatment. Indeed, we have observed in preliminary experiments that, whereas 72 hours of treatment were necessary to observe a significant difference in cytotoxic effects, 24 to 48 hours of gemcitabine treatment induced a significant gene expression.

Semiquantitative reverse transcription–PCR analysis. Total RNA extractions were performed using TRIzol reagent (Invitrogen) and treated with RNase-free Dnase I. Total RNA was reverse-transcribed and amplified by PCR. Oligonucleotides used as PCR primers are summarized in Table 1. Polymerase chain reactions for *hENT1*, *dCK*, *dCK::UMK*, *TRAIL*, and *Survivin* genes were carried out as follows: 3 minutes at 94°C, followed by 30 cycles (40 seconds at 94°C, then 40 seconds at 55°C [*dCK*], 58°C [*hENT1*, *dCK::UMK*, and *Survivin*], or 62°C [*TRAIL*], and 1 minute at 72°C) and a final extension step

Table 1. Sequences of Primers Used in RT-PCR.

Gene	Forward Primer (5′-3′)	Reverse Primer (5′-3′)
hENT1	gctgggtctgaccgttgtat	ctgtacagggtgcatgatgg
DCK	atggtaccgccaccatggccaccccg	atgtcgactcacaaagtactca
dCK::UMK	atggtaccgccaccatggccaccccg	atgcggccgcttagccttccttg
TS	aaacgtgtgttctggaaggg	ccatatctctgtattctgcc
RR	atgaaaacttggtcgagcgat	tggcaatttggaagcccataga
TRAIL	ctgagcaacgcagactcgctgtccac	tccaaggacacggcagagcctgtgccat
Bax	tgcttcagggtttcatccagg	tggcaaagtagaaaagggcga
Bcl2	aatggcaacccatcctggca	ttctcctggatccaaggctc
Survivin	atgggtgccccgacg	ctcaatccatggcagcc
GAPDH	accacagtccatgccatcac	tccaccaccctgttgctgta

(7 minutes at 72°C). Thymidylate synthase amplification conditions were as follows: 4 minutes at 94°C, 30 cycles (30 seconds at 94°C, 1 minute at 58°C, and 2 minutes at 72°C) and an extension step of 7 minutes at 72°C. For Bax and Bcl2 amplification, conditions were as follows: 3 minutes at 94°C and 30 cycles for 1 minute at 94°C, 1 minute at 58°C and 60°C for Bax and Bcl2, respectively, and 1 minute at 72°C and 10 minutes at 72°C. With regards to *RR* gene, PCR was performed as indicated: 3 minutes at 94°C and 30 cycles for 1 minute at 94°C, 40 seconds at 58°C, 1 minute at 72°C, and 7 minutes at 72°C. For *GAPDH*, PCR was incubated as followed: 3 minutes at 94°C, then 1 minute at 94°C, 45 seconds at 60°C, and 45 seconds at 72°C, repeated 34 times, and finally 5 minutes at 72°C. The experiments were repeated three times for each assay.

Western blot analysis. Cells were harvested, washed with ice-cold PBS, and lysed with RIPA buffer (Sigma-Aldrich, France). Total protein concentration was measured using the bicinchoninic acid assay kit (Sigma). Equal amounts of proteins were separated on NuPAGE Novex 4% to 12% Bis-Tris gels (Invitrogen) and transferred onto Hybond-P poly(vinylidene difluoride) membranes (Amersham Biosciences, Les Ulis, France) using a BioRad semidry transfer system. Blots were then probed overnight at 4°C with rabbit polyclonal anti–caspase-3 (1:2000), mouse monoclonal anti–poly(ADP-ribose)polymerase (PARP) (1:250), or mouse monoclonal anti–β-actin (1:2000); all antibodies were from Santa Cruz, Tebu-Bio, France. Immunoblots were developed using enhanced chemiluminescence–enhanced chemiluminescence reagents after incubating with horseradish peroxidase–conjugated secondary antibodies.

Cell Proliferation and Cytotoxic Activity

[^{3}H]Thymidine incorporation. Cells were seeded on 96-well plates and allowed to adhere overnight. Then, cells were infected with Ad-dCK or Ad-dCK::UMK (multiplicity of infection, 100) and/or transfected with TS/RRM2 siRNA (100 nM). After 24 hours, cells were further treated with different concentrations of gemcitabine (Lilly, France) for 72 hours. To determine DNA synthesis level, 1 μl of [^{3}H]thymidine (1 μCi/ml; Amersham Biotechnologies, France) was added to each well 24 hours before the end of treatment. The next day, cells were washed with PBS, fixed in ice-cold 10% trichloroacetic acid, and lysed in 0.34N NaOH. The radioactivity incorporated into the DNA was measured in triplicate by liquid scintillation spectrometry with a beta counter (Kontron, France).

MTT assay. Cell viability was evaluated using 3-[4,5-dimethylthiazol-2-yl]-3,5-diphenyl tetrazolium bromide (MTT) test. After the treatment period as indicated above, the incubation media were removed and exchanged with 100 μl of fresh media containing MTT (0.2 mg/ml), and cells were incubated at 37°C for 3 hours. The media were removed, and formazan crystals were solubilized with 150 μl of DMSO. Absorbance at 570 nm was measured in triplicate using a microplate reader (BioRad, France).

Detection of Apoptosis

Hoechst staining. Cells were seeded in four-well plates at a density of 2×10^5 cells per well. After treatment, cells were washed with PBS and fixed in 4% paraformaldehyde during 1 hour at 4°C. Cells were then stained with Hoechst reagent (1 μg/ml; Sigma) in a dark chamber at room temperature for 1 hour and examined using excitation and emission filters of 348 and 480 nm, respectively.

Caspase-3 activity. Treated cells were collected by centrifugation and washed twice with PBS. Caspase-3 activity was detected using caspase-3 colorimetric assay kit (R&D Systems, France). Cell pellets were recovered in lysis buffer, and protease activity was measured by a colorimetric reaction at a wavelength of 405 nm. Experiments were performed in triplicate and repeated three times.

Nuclear Factor-κB Transcription Analysis

DNA-binding assay. Nuclear extractions were performed on treated cells using EpiQuick Extraction Kit (Euromedex, Strasbourg, France). They were subsequently submitted to the NoShift Nuclear Factor-κB (NF-κB) transcription assay, a colorimetric assay–based alternative to electrophoretic mobility shift assay, according to the protocol instructions (Novagen, VWR, France). For quantification of activity, optical densities were measured at 450 nm with a microplate reader (BioRad, France).

NF-κB promoter activity. Transcriptional regulation of the *NF-κB* gene was determined using a NF-κB promoter/luciferase construct (NF-κB-luc; kindly provided by Professor Shinichi Kawai, Toho University School of Medicine, Tokyo, Japan). After plating overnight in a 24-well plate, cells were transiently transfected with NF-κB-luc plasmid (1 μg) using Lipofectamine 2000 reagent (Invitrogen). The next day, tumor cells were submitted to the different treatments. Thereafter, cells were harvested by gentle scraping, washed once in PBS, and resuspended in appropriate lysis buffer for subsequent analysis. Luciferase assays were performed according to the manufacturer's protocol (Promega, Charbonnières, France) using a luminometer (LUMISTAR BM6).

Pancreatic Tumor Models

Animals. Six-week-old female nude mice were purchased from Elevage Janvier (le Genest, France), housed in appropriate animal care facilities during the experimental period, and handled following the institutional guidelines required for animal experimentation.

Subcutaneous pancreatic tumor xenograft model. Mice were subcutaneously inoculated in their interscapular region with BxPc3 (1×10^7) or Panc1 (2×10^7) tumor cells. When tumors became palpable (100 mm^3), mice were randomly divided into seven groups ($n = 8$). Mice received intratumoral injection of 1×10^9 plaque-forming units

(PFUs) of Ad-dCK (G3) or Ad-dCK::UMK (G4 and G6) at days 10 and 17. In addition, they were intratumorally injected with TS and RRM2 siRNA (each 100 μg; G5, G6, and G7) at days 12 and 19. Gemcitabine (15 mg/kg) was injected intraperitoneally (IP) in G2 to G6 groups three times during 1 week. Reverse transcription–PCR (RT-PCR) experiments were performed on tumor biopsies obtained from two mice per group. Tumors were measured with calipers in three dimensions, twice a week for approximately 1 month. Tumor volumes were calculated using the formula: $v = \pi/6 \times \text{length} \times \text{height} \times \text{width}$.

Orthotopic pancreatic tumor xenograft model. Tumor cell implantation was made under surgical sterile conditions. The abdomen was cleaned with iodine solution, and a 1-cm midline incision was made to expose the pancreas. Panc1 cells (2×10^7 in 100 μl of PBS) were injected into the tail of the pancreas using a 30-gauge needle and a 1-ml disposable syringe. Abdominal wound was closed in two layers with 6-0 nylon surgical suture. Tumors were allowed to grow, and mice were then randomly assigned in five (G1-G5) treatment groups (n = 14). Mice received peritumoral injection of 1×10^9 PFU of Ad-dCK::UMK (G3 and G5) at days 10 and 17. In addition, they were peritumorally injected with TS and RRM2 siRNA (each 100 μg; G4 and G5) at days 12 and 19. Gemcitabine (15 mg/kg) was injected IP in G2 to G6 groups three times during 1 week. Six mice per group were killed at day 30, and pancreatic tumors were dissected. Volumes were measured as described above, and tumors were then fixed in Boin's solution for subsequent histologic diagnosis and immunohistochemistry analysis. The remaining animals were observed daily for survival.

Tumor morphology, immunohistochemical staining for Ki-67, and terminal deoxynucleotidyl transferase–mediated nick end labeling. Samples from tumor xenografts were dissected, fixed in Boin's solution, and then paraffin-embedded. Sections of 5 μm were realized and submitted to hematoxylin/eosin staining for morphologic examination, Ki-67 staining for proliferation study (Abcam, Paris, France), or DeadEnd Fluorometric TUNEL System (Promega) for *in situ* apoptosis study.

Statistical Analysis

Results represent means ± SEM. Differences between groups were examined for statistical significance with analysis of variance and/or the Student-Newman-Keuls test. $P < .05$ indicated a statistically significant difference.

Results

Chemosensitivity to Gemcitabine Differs in Pancreatic Tumor Cells

First, we determined the sensitivity of human pancreatic cells to gemcitabine using MTT assay. Cells were submitted for 72 hours to a range of gemcitabine concentrations going from 0.01 to 100 μM. HA-hpc2 cells showed the highest sensitivity to gemcitabine with a half maximal inhibitory concentration (IC_{50}) equal to 0.01 μM. BxPc3 and Panc1 cells exhibited intermediate (IC_{50} = 2 μM) and low (IC_{50} = 40 μM) sensitivity, respectively (Figure 1*A*). Thus, we defined HA-hpc2 and BxPc3 as sensitive tumor cells; and Panc1, as resistant tumor cells. To investigate the improvement of gemcitabine antitumor effect by TS/RRM2 siRNA and Ad-dCK::UMK combination strategy, the rest of the study was performed on the Panc1-resistant cells. The BxPc3, gemcitabine-sensitive tumor cells that are highly susceptible to respond to the combined strategy, were used as positive control.

Variations in Gemcitabine Sensitivity Are Related to Its Metabolic Gene Expression

Several studies have demonstrated that tumor cell resistance to gemcitabine can be related to a defect of gemcitabine transport [30] and especially to a deficit of the *hENT1* predominant nucleoside transporter. To verify this option, we determined the level of *hENT1* expression and its correspondent activity in gemcitabine-treated and -untreated BxPc3 and Panc1 cells. Our data showed that basal *hENT1* messenger RNA (mRNA) levels were unexpectedly slightly more marked in the Panc1-resistant cells (Figure 1*B*) and increased in both cell lines after a 48-hour period of gemcitabine treatment. Thereafter, to verify *hENT1* involvement in gemcitabine cytotoxicity, *hENT1*-related transport activity was inhibited using nitrobenzylthioinosine (NBTI). Tumor cells were incubated with NBTI (10 and 100 nM) in the presence of increasing concentrations of gemcitabine for 72 hours. As indicated in Figure 1*C*, BxPc3 gemcitabine-related cell death was inhibited in a dose-dependent manner. On the contrary, NBTI treatment didn't affect Panc1 cells viability. In parallel, we studied the expression of different gemcitabine-related metabolic genes. Whereas basal expression of dCK was more important in HA-hpc2 and BxPc3 cells, TS and RR expressions were higher in Panc1 cells (Figure 1*D*). After a 48-hour period of gemcitabine treatment, the gene expression profile remained unchanged in BxPc3 and HA-hpc2 and was, on the contrary, emphasized in Panc1 with a more marked decrease of *dCK* mRNA and an increase of *RR* and *TS* mRNA. Thus, Panc1 tumor cell resistance to gemcitabine seems to be due, at least in part, to alteration in drug metabolism.

Ad-dCK::UMK and TS/RRM2 siRNA Increase Gemcitabine Cytotoxicity In Vitro

Considering the decrease of dCK expression, the dramatic increase of TS, and, to a lower extent, the increase of RR expression in Panc1 cells, an adenovirus overexpressing dCK::UMK and siRNA targeting *TS* and *RR* genes were used to favor gemcitabine phosphorylation. Infection of BxPc3 and Panc1 cells with Ad-dCK::UMK for 48 hours resulted in dCK and dCK::UMK overexpression, when compared with noninfected control cells. In the same way, the endogenous expression of RR and TS observed in the nontransfected control cells was downregulated in cells treated with the appropriate siRNA for 48 hours (Figure 2*A*). Growth inhibition studies using [^{3}H]thymidine incorporation assay indicated that inhibition of DNA synthesis generated by gemcitabine was increased in BxPc3 and Panc1 cells preinfected with Ad-dCK::UMK ($P < .001$ *vs* gemcitabine-treated cells) or pretreated with the combination of TS and RRM2 siRNA ($P < .001$ *vs* gemcitabine-treated cells), particularly in Panc1 cells. This more marked retardation of cell proliferation resulted in a better cytotoxicity of gemcitabine. Indeed, overexpression of dCK::UMK fusion gene contributed to reduce approximately five and seven times the gemcitabine IC_{50} in BxPc3 ($P < .001$ *vs* gemcitabine-treated cells) and Panc1 ($P < .001$ *vs* gemcitabine-treated cells) cells, respectively. Likewise, inhibition of TS/RR expression reduced gemcitabine IC_{50} from 2 and 40 μM to 0.5 and 5 μM, respectively, in BxPc3 ($P < .001$ *vs* gemcitabine-treated cells) and Panc1 cells ($P < .001$ *vs* gemcitabine-treated cells; Figure 2*B*). The IC_{50} data of [^{3}H]thymidine incorporation assays seemed to be slightly lower than those described in MTT assays. The observed discrepancy can be explained by the delay

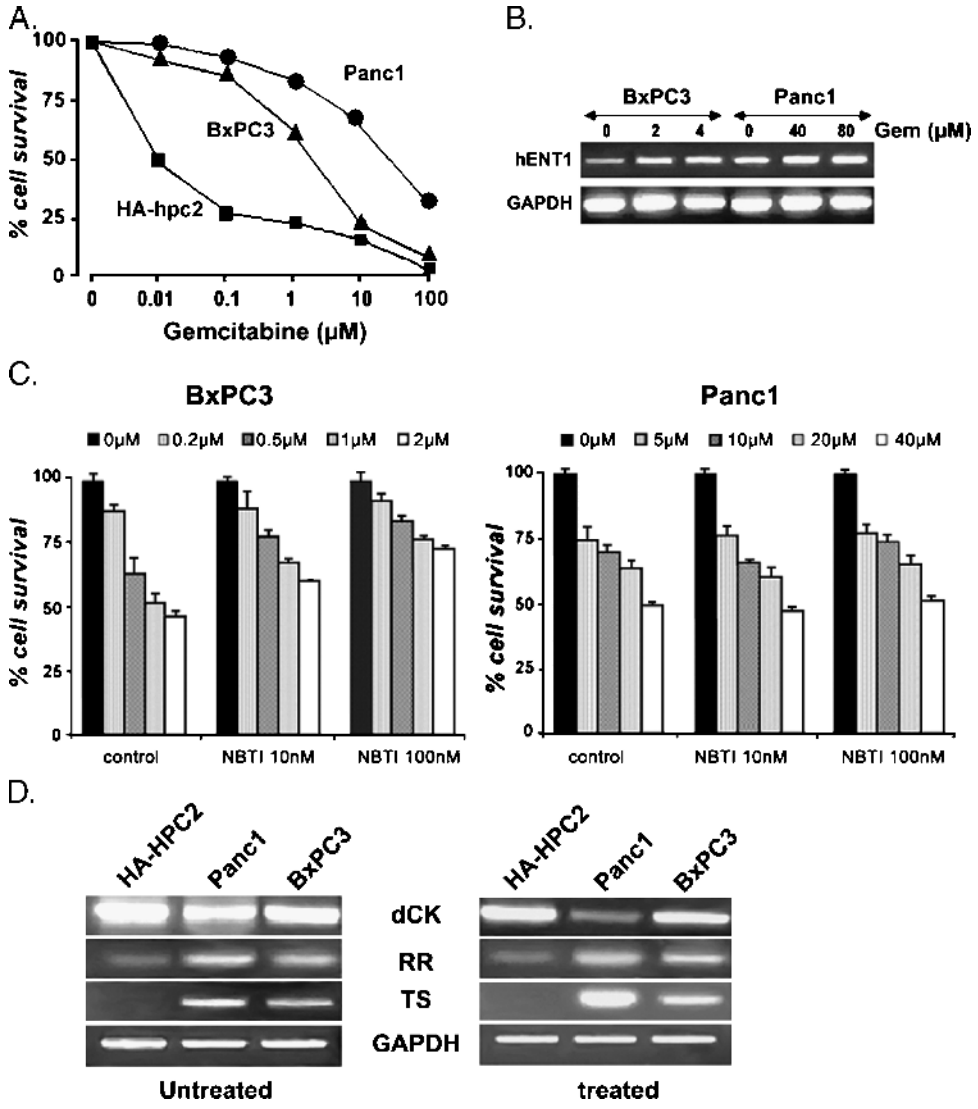

Figure 1. Pancreatic tumor cells sensitivity to gemcitabine. (A) Gemcitabine cytotoxicity. Panc1, BxPc3, and HA-hpc2 cells were treated for 72 hours with increasing concentrations of gemcitabine (0.01-100 μM). Cell viability was measured using MTT test and was presented as a percentage of untreated cell control values. Each curve is representative of four experiments performed in triplicate. (B) Expression of the *hENT1* nucleoside transporter. Cells were untreated or treated with gemcitabine for 48 hours, and RNA was extracted and submitted to RT-PCR analysis using specific primers for *hENT1* and *GAPDH* housekeeping gene. (C) Role of *hENT1* in gemcitabine transport. BxPc3 and Panc1 cells were treated simultaneously with gemcitabine and the hENT1 inhibitor NBTI (10 and 100 nM). Three days later, cell survival was evaluated by MTT assays. (D) Expression of *dCK*, *RR*, and *TS*. Tumor cells were untreated or treated with gemcitabine at IC_{50} concentrations, and mRNA levels were evaluated 48 hours later using semiquantitative RT-PCR with specific primers.

between the time course of DNA synthesis arrest and the implementation of cell death mechanisms.

Ad-dCK::UMK and TS/RRM2 siRNA Treatments Favor Gemcitabine-Induced Apoptosis and Are Mainly Associated with an Increase of TRAIL Expression

Gemcitabine failure can be due to defects in apoptosis pathways. Thus, we next examined whether association of Ad-dCK::UMK or TS/RRM2 siRNA would influence the responsiveness of pancreatic tumor cells to gemcitabine-induced apoptosis. Western blot analysis revealed that the slight 85-kDa PARP cleavage product observed after gemcitabine treatment *per se* was augmented in BxPc3 and Panc1 cells pretreated with either Ad-dCK::UMK or TS/RR siRNA (Figure 3*A*). Panc1 cells either infected with Ad-dCK::UMK or transfected with TS/RRM2 siRNA presented an increase of gemcitabine-mediated caspase-3 activation, 348 AU ($P < .001$ *vs* gemcitabine-treated cells) and 375 AU ($P < .001$ *vs* gemcitabine-treated cells), respectively (Figure 3*B*). In addition, these increases of caspase-3 activity were more important than those observed in the BxPc3-sensitive model, in which gemcitabine-related caspase-3 activity was augmented from less than 150 to 275 AU ($P < .01$ *vs* gemcitabine-treated cells) in the presence of Ad-dCK::UMK overexpression and to 298 AU ($P < .01$ *vs* gemcitabine-treated cells) after *TS*/*RRM2* gene silencing. These results were confirmed by Western blot analysis as demonstrated by the higher intensity of the cleaved forms of caspase-3 (Figure 3*A*). Caspases' activity is regulated by the inhibitors of apoptosis proteins, which determine them for degradation. Among these inhibitors, *Survivin* was

increased in tumor cells receiving gemcitabine treatment, when compared with untreated control cells. Pretreatment with either Ad-dCK::UMK or TS/RRM2 siRNA resulted in an obvious inhibition of the gemcitabine-related upregulated *Survivin* (Figure 3*C*).

We next looked for the involvement of the main mediators of extrinsic and intrinsic apoptotic pathways. Hence, we examined whether TRAIL and Bax expressions were modified in gemcitabine-induced apoptosis. Preinfection with Ad-dCK::UMK or transfection with TS/RRM2 siRNA resulted in an enhancement of TRAIL expression that seems to be equivalent in BxPc3 and Panc1 cells. Conversely, a slightly augmented Bax expression and a weak reduction of Bcl2 expression were observed in such treated cells (Figure 3*C*).

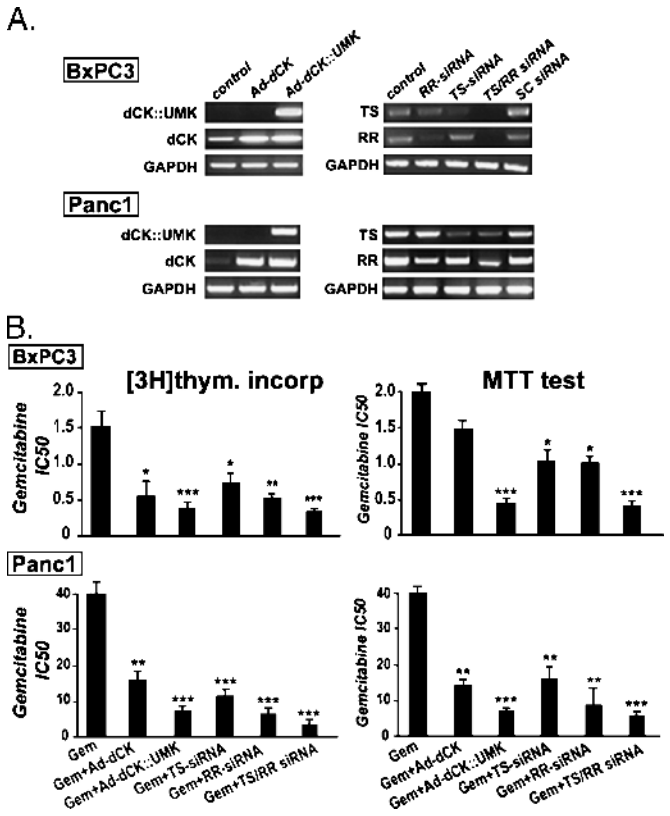

Figure 2. Combination of gemcitabine with Ad-dCK::UMK or TS/RRM2 siRNA improves gemcitabine cytotoxic apoptotic effect. (A) Efficacy of recombinant adenovirus transduction and siRNA transfection. BxPc3 and Panc1 cells were either infected with adenoviruses expressing dCK or dCK::UMK or transfected with TS and/or RRM2 siRNA. The RT-PCR analysis was carried out after a 48-hour treatment period on the total RNA using specific primers. dCK, dCK::UMK, RR, and TS expressions were compared with untreated control cells. The nonspecific scramble (Sc) siRNA was used as a negative control for siRNA. (B) Effect of Ad-dCK::UMK and TS/RRM2 siRNA on gemcitabine cytotoxicity. Cells were treated as described above and further received increasing concentrations of gemcitabine for 72 hours. In [^{3}H]thymidine incorporation and MTT assays, results of gemcitabine combined treatments are relative to Ad-dCK::UMK, TS, and/or RR siRNA treatments. The average percentage values obtained in cells treated with gemcitabine alone are relative to those of untreated cells. Values represent the mean of four experiments performed in triplicate. Asterisks indicate significant difference (*$P < .05$, **$P < .01$, and ***$P < .001$) observed after the various combined treatments when compared with gemcitabine alone.

Association of TS/RRM2 siRNA with Ad-dCK::UMK Promotes a Maximal Increase of Gemcitabine Efficacy in Tumor Cell Cultures

To obtain an optimal efficacy of gemcitabine, we finally studied the simultaneous use of Ad-dCK::UMK and TS/RRM2 siRNA. As expected, MTT assays showed that in tumor cells receiving concomitantly Ad-dCK::UMK and TS/RRM2 siRNA, gemcitabine IC_{50} was further reduced to 0.1 and 1 μM in BxPc3 and Panc1 cells, respectively (Figure 4*A*). Gemcitabine at 1 μM caused 54% of cell death in Panc1 cells previously treated with Ad-dCK::UMK plus TS/RRM2 siRNA ($P < .001$ *vs* gemcitabine-treated cells), whereas being not effective when used alone. Treatment with either Ad-dCK::UMK ($P < .05$ *vs* gemcitabine-treated cells) or TS/RRM2 siRNA ($P < .01$ *vs* gemcitabine-treated cells) increased gemcitabine's cytotoxic effect to a lower extent. At the same concentration, gemcitabine induced 78% of cell death in BxPc3 treated with Ad-dCK::UMK plus TS/RRM2 siRNA ($P < .001$ *vs* gemcitabine-treated cells). However, this enhanced cytotoxic effect of gemcitabine on BxPc3 cells was, nevertheless, near equivalent to that obtained with Ad-dCK::UMK ($P < .001$ *vs* gemcitabine-treated cells) or TS/RRM2 siRNA ($P < .001$ *vs* gemcitabine-treated cells) alone. For apoptosis analysis, Hoechst staining demonstrated an augmentation of nuclear shrinkage and chromatin condensation and fragmentation (Figure 4*B*). ELISA experiments showed in both BxPc3-sensitive cells and Panc1-resistant cells treated with the tritherapy a more marked activation of caspase-3 ($P < .001$ *vs* gemcitabine-treated cells) that was furthermore significantly higher than that generated by the association of gemcitabine with either Ad-dCK::UMK ($P < .01$ *vs* gemcitabine + Ad-dCK::UMK–treated cells) or TS/RRM2 siRNA ($P < .001$ *vs* gemcitabine + TS/RRM2 siRNA–treated cells; Figure 4*C*). Increase of caspase-3 activity was confirmed by the higher levels of the two caspase-3 cleaved isoforms of 17 and 20 kDa. In addition, we observed an enhanced *TRAIL* expression and a higher inhibition of *Survivin* and *Bcl2* expression. Concerning *Bax* proapoptogene, a slightly enhanced expression was observed with the combined treatment (Ad-dCK::UMK + TS/RRM2 siRNA + gemcitabine; Figure 4*D*). Several authors reported that gemcitabine-resistant cells exhibited high basal and induced NF-κB activity [31]. Thus, we next wanted to determine the involvement of NF-κB in the enhancement of gemcitabine efficacy by the association Ad-dCK::UMK plus TS/RRM2 siRNA. The role of NF-κB was thus ascertained using the NoShift NF-κB assay and a luciferase reporter gene assay. As shown in Figure 5, gemcitabine alone increased NF-κB activity particularly in Panc1 cells ($P < .05$ *vs* nontreated cells). Interestingly, the combination of Ad-dCK::UMK plus TS/RRM2 siRNA significantly reduced the gemcitabine-induced active NF-κB ($P < .001$ *vs* gemcitabine-treated Panc1 cells).

In Vivo *Experiments*

Having shown that combined modalities using Ad-dCK::UMK and TS/RR siRNA improve gemcitabine activation and effectiveness *in vitro*, particularly in the chemoresistant Panc1 tumor cells, we next examined *in vivo* efficacy using BxPc3 and Panc1 tumor xenograft models in immune-deficient mice.

Combination of gemcitabine with Ad-dCK::UMK plus TS/RRM2 siRNA inhibits subcutaneous tumor xenograft growth. To determine a comparative efficacy of the tritherapy strategy on gemcitabine-sensitive and -resistant tumor models, BxPc3 and Panc1 subcutaneous tumor models were established. The treatment protocols were initiated with comparable tumor volumes in both BxPc3 and Panc1 tumor–bearing mice (approximately 100 mm^3, as indicated in the

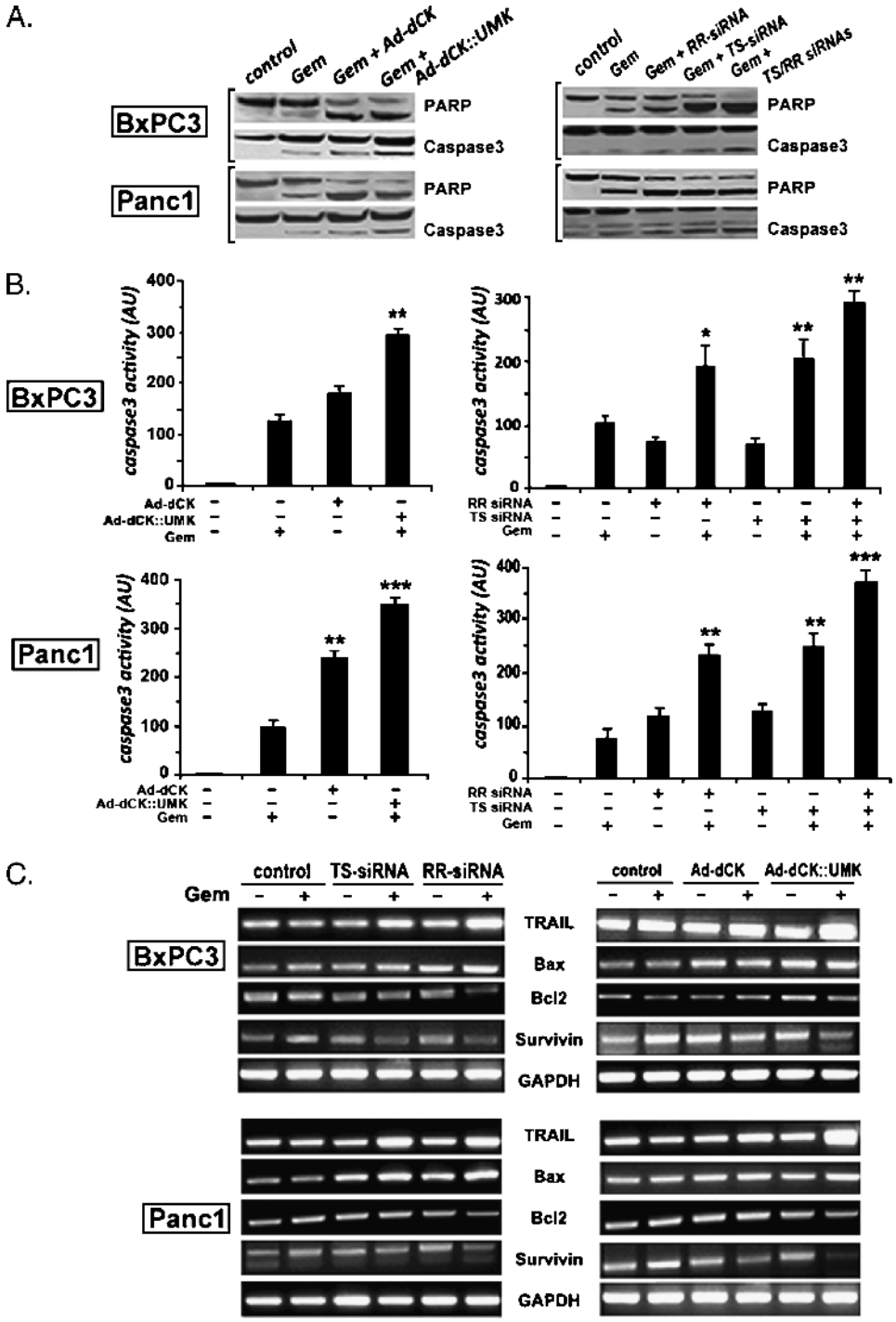

Figure 3. Combination of gemcitabine with Ad-dCK::UMK or TS/RRM2 siRNA improves gemcitabine cytotoxic apoptotic effect. (A) Enhancement of PARP and caspase-3 activation. To assess PARP and caspase-3 activation, Western blot analysis experiments were performed on cell lysates obtained from cells treated with either Ad-dCK::UMK or TS/RRM2 siRNA and further treated with gemcitabine (IC_{50} doses) during 48 hours. The upper panels represent the 116-kDa native form and the 85 kDa activated form of PARP. The lower panels illustrate the native and the cleaved forms of caspase-3 (17 and 20 kDa). (B) Quantitative measurement of caspase-3 activity. Caspase-3 activation was also evaluated by colorimetric assays. Data are representative of three independent experiments. Asterisks indicate significant difference (**$P < .01$ and ***$P < .001$) observed after the various treatments when compared with gemcitabine alone. (C) Expression study of different apoptotic genes. Treated cells were submitted to gemcitabine treatment for 48 hours and then used for *TRAIL*, *Bax*, *Survivin*, and *Bcl2* mRNA level measurement using RT-PCR analysis. *GAPDH* was used as an internal control.

Materials and Methods section). First, to determine the efficacy of the recombinant adenovirus transduction and siRNA transfer, we performed RT-PCR experiments and analyzed the expression of the target genes in tumor biopsies recovered at day 21. As shown in Figure 6*A*, *dCK::UMK* fusion gene was highly expressed in tumor tissues obtained from mice treated with Ad-dCK::UMK alone or combined to TS/RRM2 siRNA. Expression of *TS* and *RR* genes was inhibited in biopsies from TS/RRM2 siRNA and TS/RRM2 siRNA plus Ad-dCK::

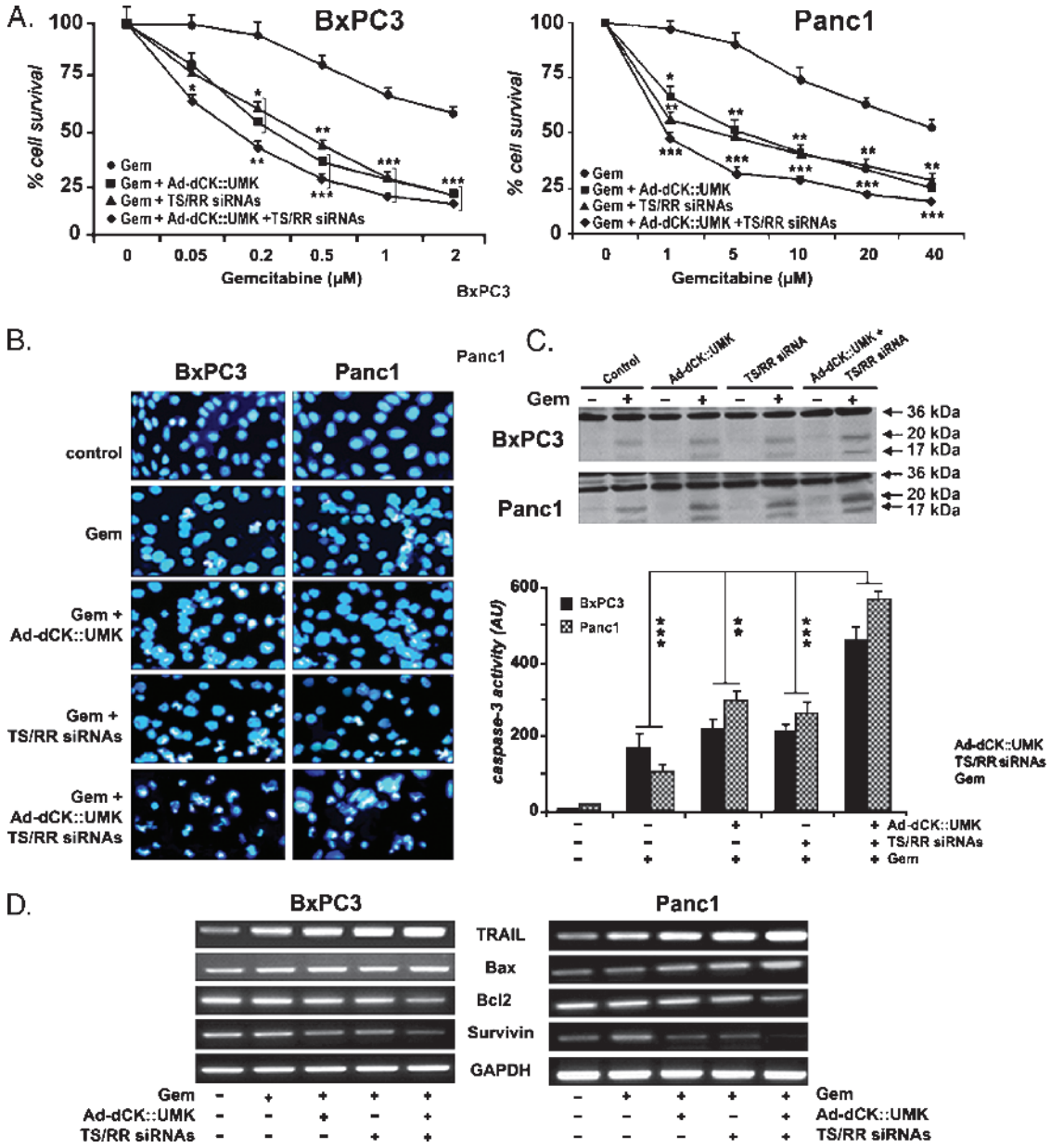

Figure 4. Maximal optimization of gemcitabine efficacy is obtained by combination with Ad-dCK::UMK and TS/RR siRNA. (A) Cytotoxic effect of Gemcitabine combination with Ad-dCK::UMK and TS/RR siRNA. Cell viability was determined on Ad-dCK::UMK–infected and/or TS/RR siRNA–transfected cells by MTT assay after 72 hours of treatment with increasing concentrations of gemcitabine. The average percentages of the MTT value obtained in gemcitabine-treated cells are relative to those of untreated cells. Concerning the gemcitabine combined treatments, results represent relative value of gemcitabine-combined treatments to Ad-dCK::UMK, TS/RR siRNA, or Ad-dCK::UMK plus TS/RR siRNA treatments. Data are the result of three independent experiments. Asterisks indicate significant difference (*$P < .05$, **$P < .01$, and ***$P < .001$) observed after the various treatments when compared with gemcitabine alone. (B) Hoechst staining. Cells were treated as indicated in the Materials and Methods section. Apoptotic cells were visualized using fluorescent microscope. (C) Caspase-3 activation. Activity of caspase-3 was studied by Western blot analysis and colorimetric activity assay on cells having received Ad-dCK::UMK plus TS/RRM2 siRNA and further treated for 48 hours with gemcitabine at IC_{50} doses. Asterisks indicate significant difference (**$P < .01$ and ***$P < .001$) observed after cell treatment with gemcitabine associated to both Ad-dCK::UMK and TS/RR siRNA treatments compared with cells treated with gemcitabine plus Ad-dCK::UMK or gemcitabine plus TS/RRM2 siRNA. (D) Expression of apoptotic mediators. In the same experiment, *TRAIL*, *Bax*, *Bcl2*, and *Survivin* apoptotic gene expressions were evaluated by RT-PCR experiments using their respective specific primers. The expression of *GAPDH* is shown as an internal control.

UMK–treated mice. Second, concerning the treatment efficacy, as expected, BxPc3 tumor model responded efficiently to gemcitabine ($P < .01$ *vs* nontreated BxPc3-bearing mice), which was not the case of the chemoresistant Panc1 tumor model (NS; Figure 6*B*). At the end of the experiment, the concomitant association of Ad-dCK::UMK and TS/RRM2 siRNA with gemcitabine reduced tumor volumes by 66% and 78% ($P < .001$), respectively, in BxPc3 and Panc1 tumor models, when compared with mice treated with gemcitabine alone. Furthermore, in comparison to the dual-therapy regimens, the tritherapy generated 57% ($P < .05$) and 48% ($P < .05$) of Panc1 tumor volume

diminution when compared with mice treated with gemcitabine plus Ad-dCK::UMK and gemcitabine plus TS/RRM2 siRNA, respectively. Importantly, in the mean time, these inhibitions were higher than those observed in BxPc3-sensitive tumor model, in which 39% (NS *vs* gemcitabine + Ad-dCK::UMK–treated mice) and 31% (NS *vs* gemcitabine + TS/RRM2 siRNA–treated mice) of tumor inhibition were observed.

Gemcitabine-based combination therapy delays tumor growth and prolongs survival of mice bearing orthotopic pancreatic cancer xenografts. Taking in account the appropriate tumor microenvironment, the *in vivo* investigation was extended to a much more predictive orthotopic pancreatic cancer Panc1 model. Tumor extension was determined by explorative laparotomy ($n = 6$) 30 days after tumor establishment. Figure 7*A* summarizes tumor growth evolution showing that mice treated with gemcitabine alone have a mean tumor volume of 839 mm^3 *versus* 1260 mm^3 in control mice (33% reduction of tumor growth, NS *vs* untreated control mice). Gemcitabine plus TS/RRM2 siRNA treatment reduced the tumor volume to 398 mm^3, corresponding to a mean 68% reduction of tumor volume ($P < .01$ *vs* gemcitabine-treated mice). Treatment with gemcitabine plus Ad-dCK::UMK resulted in a mean 65% reduction of tumor volume (446 mm^3, $P < .01$ *vs* gemcitabine-treated mice). As expected, mice having received gemcitabine treatment combined with TS/RRM2 siRNA and Ad-dCK::UMK demonstrated the greatest inhibition of tumor growth and bore an average tumor volume of 151.02 mm^3 resulting in a mean 82% decrease of tumor growth ($P < .001$ *vs* gemcitabine). Furthermore, combined treatment significantly prolonged survival of mice. Half of the mice receiving gemcitabine and Ad-dCK::UMK in combination were alive and exhibited a healthy appearance. Moreover, combination of TS/RRM2 siRNA to gemcitabine treatment prolonged survival of mice by 62% ($P < .01$ *vs* gemcitabine-treated mice). The most important prolongation of survival was observed in mice treated with gemcitabine combined to Ad-dCK::UMK and TS/RRM2 siRNA, with seven of eight mice still alive at the end of 3 months of experiment ($P < .001$ *vs* gemcitabine-treated mice; Figure 7*D*). Tumor tissues were subjected to *in situ* apoptosis examination (Figure 7*C*). Terminal deoxynucleotidyl transferase–mediated nick end labeling (TUNEL)–positive cells were most prominent in tumor biopsies obtained from animals

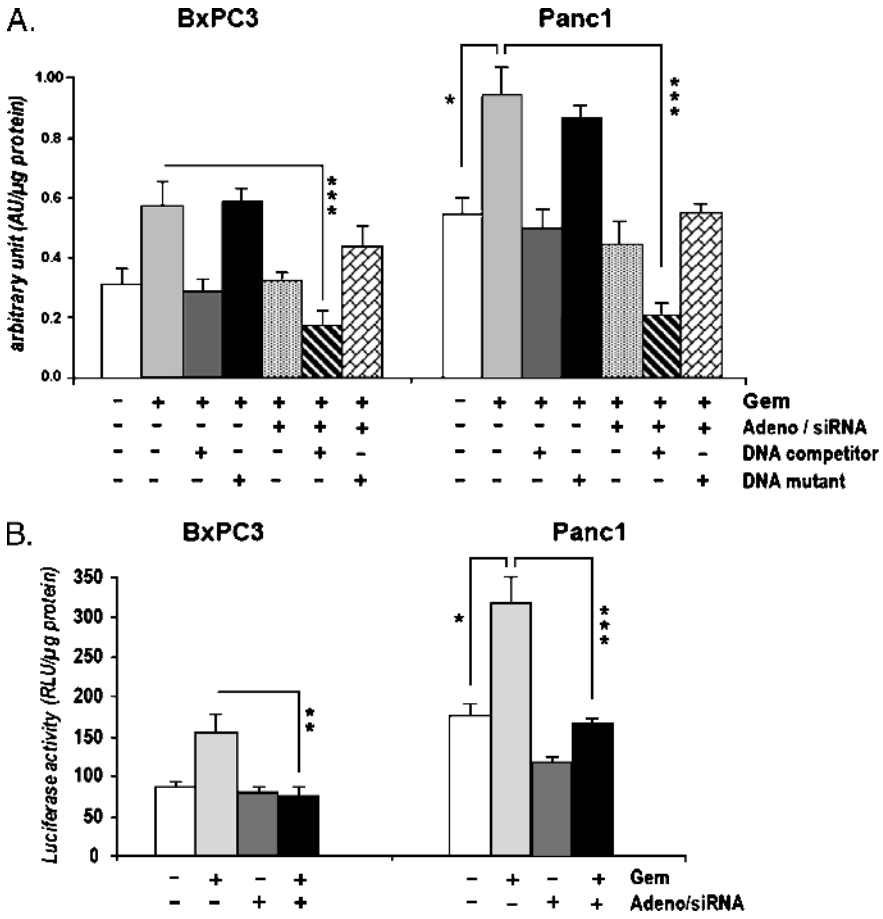

Figure 5. Role of NF-κB in tumor cell sensitivity to gemcitabine alone or in combination with Ad-dCK::UMK and TS/RRM2 siRNA. BxPc3 and Panc1 tumor cells were cotreated with Ad-dCK::UMK and TS/RR siRNA. One day later, cells further received 2 and 40 μM of gemcitabine, respectively, and NF-κB activation was studied after 48 hours. (A) NoShift NF-κB colorimetric assay. Cells were harvested, and NF-κB activity was evaluated according to the manufacturer's recommendations. (B) NF-κB luciferase gene reporter assay. Herein, cells were primary transfected with a plasmid-expressing luciferase under control of an NF-κB response element. Luciferase assays were then performed according to the manufacturer's protocol. All experiments were performed in triplicate and repeated at least three times. Asterisks indicate significant difference (**$P < .01$ and ***$P < .001$) observed in cells treated with the tritherapy gemcitabine plus Ad-dCK::UMK plus TS/RR siRNA compared with cells treated with gemcitabine alone. *$P < .05$ indicates the significant difference observed between gemcitabine-treated Panc1 cells relative to untreated Panc1 cells.

treated with Ad-dCK::UMK and TS/RRM2 siRNA in combination with gemcitabine, when compared with mice treated with gemcitabine alone. Protease activity analyzed by Western blot showed that caspase-3 activation after exposure to gemcitabine was significantly increased in tumors of mice receiving the combined treatment (data not shown). No apoptosis was seen in healthy pancreas biopsies, in which no caspase-3 cleavage was observed (data not shown). In addition, we evaluated the tumor proliferative activity. As shown in Figure 7*C*, tumor biopsies from mice treated with the "three-therapy" protocol have a reduced number of Ki-67–positive tumor cells in comparison to tumors from gemcitabine-treated animals.

Discussion

The focus of the present work was to investigate the molecular modulation of gemcitabine metabolism and to improve its antitumor cytotoxic effect. Thus, to provide new insight into pancreatic cancer treatment, we have performed a strategy combining GDEPT system and siRNA-based methodology. Our approach was motivated by the hypothesis that gemcitabine resistance may be dependent on decreased expression of *dCK* and/or overexpression of *RR* and *TS*. Recent studies have reported that the ratio of expression of these genes could be responsible for the acquired and inherent chemoresistance of pancreatic cancer cells to gemcitabine [32].

In the current study, the sensitivity of different pancreatic tumor cell lines to gemcitabine corroborated other data reported elsewhere and characterized Panc1 and BxPc3 cells as resistant and sensitive cells, respectively [33,34]. Nevertheless, variations of IC_{50} were observed due to the different experimental conditions from laboratory to another. In many studies, the proposed mechanisms of chemoresistance to nucleoside analogs are the low levels of proteins implicated in drug transport or the dysregulation of intracellular enzymes (e.g., kinases, deaminases, and nucleotidases) responsible for their metabolism [15,21,26]. Thus, quite logically, we next attempted to analyze gemcitabine transporters and especially the *hENT1* transporter, which deficiency was correlated to lack of gemcitabine transport

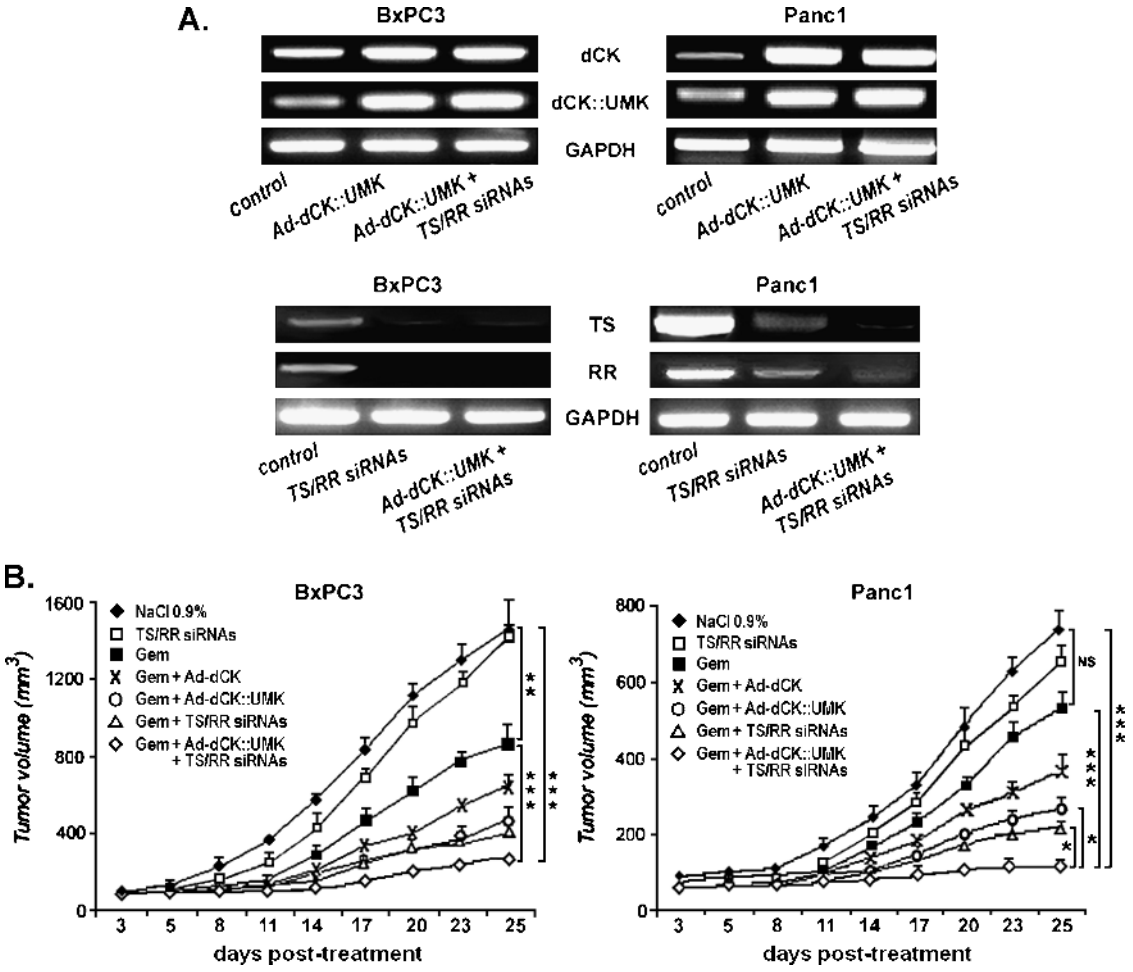

Figure 6. Overexpression of dCK::UMK and down-regulation of TS/RR improved gemcitabine's therapeutic effect in subcutaneous pancreatic tumor models. Nude mice were subcutaneously inoculated with BxPc3 or Panc1 cells, and when their tumor size reached 100 mm^3, they received intratumor injection of Ad-dCK::UMK (1×10^9 PFU) ± TS/RR siRNA (100 μg). Gemcitabine (15 mg/kg body weight) was administrated intraperitoneally. Control group was treated with 0.9% NaCl. (A) Ad-dCK::UMK and TS/RR siRNA functionality. Tumors were recovered from two mice per group, and RT-PCR experiments were carried out to demonstrate the reduction of endogenous TS and RR expression and the overexpression of dCK and dCK::UMK after siRNA and Ad-dCK::UMK treatments, respectively. *GAPDH* was used as an internal control. (B) Tumor growth. Tumor growth evolution of BxPc3 and Panc1 tumors was followed up by tumor volume measurement two times weekly. *NS* indicates not significant. $^{**}P < .01$ and $^{***}P < .001$ *versus* control.

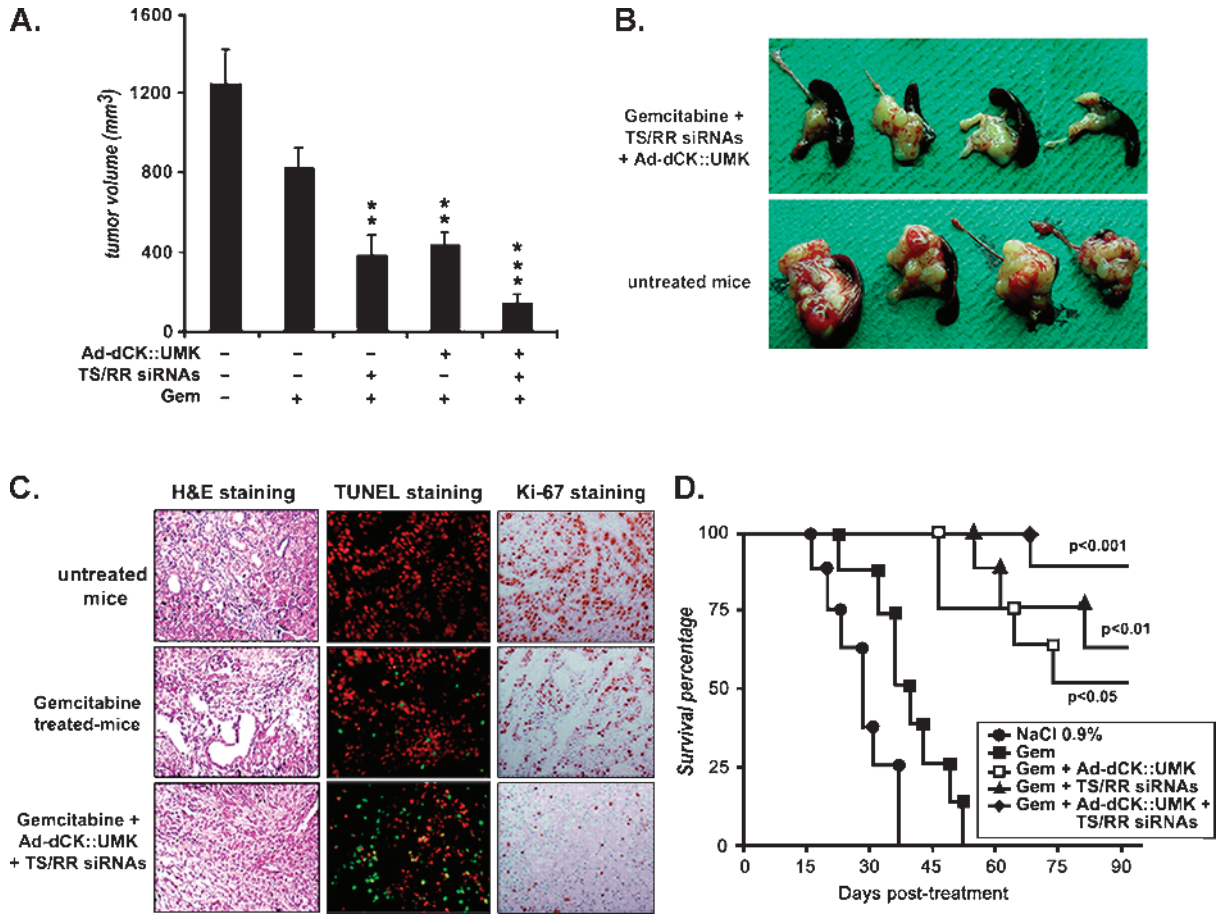

Figure 7. Inhibition of orthotopic tumor formation and increased survival of tumor-bearing mice after combined gemcitabine-based treatment. Thirty days after the beginning of treatment, six mice from each group ($n = 14$) were killed; their pancreatic tumors were recovered. (A) Tumor growth. Recovered biopsies were measured in three dimensions. Asterisks indicate significant difference (**$P < .01$ and ***$P < .001$) observed after gemcitabine combined treatments compared with gemcitabine alone. (B) Macroscopic findings of pancreas. Photographs represent excised pancreatic tumor from untreated mice and those receiving tritherapy protocol. (C) Representative immunohistochemistry examination. Biopsies were subsequently submitted to hematoxylin-eosin staining (left panels), TUNEL staining (middle panels), and Ki-67 staining (right panels). (D) Kaplan-Meier survival curve. Remaining mice were followed for survival curve determination. Results were analyzed statistically by log-rank test. Asterisks indicate significant difference (*$P < .5$, **$P < .01$, and ***$P < .001$) observed after gemcitabine combined treatments compared with gemcitabine alone.

and chemoresistance [30]. Our findings indicated that inhibition of the *hENT1*-mediated transport by NBTI modestly modifies gemcitabine activity on BxPc3 and does not alter gemcitabine cytotoxicity on the resistant Panc1 cells. Furthermore, RT-PCR experiments demonstrate augmentation of *hENT1* expression after gemcitabine treatment in both BxPc3 and Panc1 cells. Thus, BxPc3 and Panc1 sensitivity to gemcitabine does not seem to involve the *hENT1* transporter.

We next addressed the question concerning the modulation of the expression of cellular enzymes involved in gemcitabine metabolism and its correlation with chemoresistance mechanisms. It is well established that gemcitabine phosphorylation by dCK is the rate-limiting step of gemcitabine prodrug activation because dCK deficiency is critically involved in acquired resistance [16–18]. Several data showed a clear correlation between dCK activity and sensitivity of human tumor cells to gemcitabine. In this study, the basal dCK expression was significantly lower in Panc1-resistant cells compared with BxPc3- or HA-hpc2-sensitive cells and was further downregulated after exposure to gemcitabine. To overcome this situation, reexpression of dCK in drug-resistant tumor cells is generally realized. However, transfer of dCK alone does not result in complete restoration of gemcitabine sensitivity [19,20]. Thus, we considered that the design of a recombinant adenovirus expressing *dCK::UMK* fusion gene might be more efficient for pancreatic tumor chemosensitization to gemcitabine. As expected, we demonstrated that dCK::UMK expression resulted in a more marked increase of cell sensitivity to gemcitabine than did reexpression of dCK alone. These data were illustrated by the significant inhibition of DNA synthesis and cytotoxic effects. We demonstrated that the designed Ad-dCK::UMK reduced six and eight times gemcitabine IC_{50}, respectively, in BxPc3 and Panc1 cells. In addition, regarding gemcitabine metabolism and tumor sensitivity, transcriptome analysis also suggested the predictive value of RR and TS in chemoresistance mechanisms. In fact, there is accumulating data indicating the correlation between clinical response and *dCK*, *TS*, and *RR* gene expression levels in treated patients [27,32,35]. In the present study, we showed that gemcitabine treatment induced a strong increase of *RR* and *TS* expression in Panc1-resistant tumor cells and, at the same time, no significant modification in BxPc3 and HA-hpc2. Thus, the increase of TS and RR expression could be responsible, at least in part, for the low

response of Panc1 tumor cells to gemcitabine treatment. Augmentation of TS expression is not surprising because experimental and clinical studies observed an induction of TS expression after exposure to TS inhibitors, a process that leads to the development of cellular drug resistance to these agents [36]. On the basis of these findings and others reported elsewhere, we attempted to block TS and RR expression using TS/RRM2 siRNA. We observed that *TS/RRM2* gene silencing was associated with an increase of the cytotoxic effect induced by gemcitabine. It seems that TS/RRM2 siRNA were as effective as Ad-dCK::UMK at reducing gemcitabine IC_{50} as indicated by the statistical analysis realized in comparison to gemcitabine treatment. These findings confirmed clearly the crucial role of TS and RR in gemcitabine chemotherapy efficacy. Moreover, it was reported that inhibition of TS and RRM2 expression might result in a stimulation of dCK activity that may be consistent with feedback activation in response to inhibition of DNA synthesis and DNA damage [37].

Thus, ultimately to reinforce its metabolism and to optimize as much as possible its antitumor activity, gemcitabine was used in combination with Ad-dCK::UMK and the specific TS/RRM2 siRNA. Combination of these two therapeutic strategies based on gene therapy led to a 40-times decrease of gemcitabine IC_{50} in Panc1 cells (1 *vs* 40 μM in Panc1-nontreated cells), in comparison with the 7- and 8-times decrease obtained after combination of gemcitabine with Ad-dCK::UMK and TS/RRM2 siRNA treatments, respectively. Although Panc1 cells still remained more resistant than BxPc3 cells (gemcitabine IC_{50} equal to 1 μM in Panc1 cells *vs* 0.1 μM in BxPc3 cells), diminution of gemcitabine IC_{50} generated by the tritherapy was superior to that obtained in BxPc3-sensitive cells (a 20-fold decrease of IC_{50}).

Several studies have provided evidence that chemotherapeutic agents induce apoptotic tumor cell death. Recent findings suggest that diminished apoptosis plays an important role in the resistance of tumor cells to anticancer agents [38,39]. Few studies described the comprehension of gemcitabine-related apoptosis, and little is known about the apoptotic mediators involved in gemcitabine cytotoxic effect. So, in the current study, in attempting to verify any correlation between tumor chemosensitization to gemcitabine and apoptosis induction, we looked for the involvement of some of the main mediators of both extrinsic and intrinsic apoptotic pathways. Our data demonstrate that combination of gemcitabine with the two other strategies induced a significant increase of PARP cleavage and caspase-3 activation compared with gemcitabine alone. This augmented activity of caspase-3 may be explained by diminution of the Survivin inhibitor of apoptosis protein expression, which was near completely inhibited in Panc1-resistant tumor cells. In the same way, the combined treatment was associated with decrease of the antiapoptotic mediator Bcl2 expression and augmentation of Bax expression. Concerning the death receptor pathway, the contribution of the Fas/FasL death receptor pathway in gemcitabine-induced apoptosis has been a subject of controversy [40,41]. To gain further insight into the mechanisms by which the tritherapy promotes apoptosis, we investigated the *TRAIL* ligand pathway. It was already demonstrated that combination of *TRAIL* gene therapy and chemotherapy has proved to be effective against various cancer diseases [42,43]. Our finding indicated that tumor cell sensitization to gemcitabine with Ad-dCK::UMK, TS/RRM2 siRNA, or both resulted in a critical enhancement of TRAIL expression. These data suggest that the improved tumor cell sensitization to gemcitabine involved TRAIL contribution for apoptosis induction. Finally, another apoptotic pathway that could be involved in gemcitabine chemoresistance is NF-κB pathway. In fact, previous reports have demonstrated that constitutive NF-κB activity is present in approximately 70% of human pancreatic cancer and several pancreatic carcinoma cell lines [31,44–46]. Herein, we confirmed the involvement of NF-κB activity in the tumor cell's resistance to gemcitabine. Moreover, the efficacy of the tritherapy protocol was showed to occur through a reduction of the gemcitabine-related induction of NF-κB transcriptional activity. Future studies on the role of apoptosis signaling molecules in pancreatic cancer chemosensitization and treatment efficacy need more investigation.

To validate the results of *in vitro* experiments, subcutaneous and orthotopic xenograft pancreatic cancer models were initiated in athymic mice. In the subcutaneous tumor models, the simultaneous association of *Ad-dCK::UMK* overexpression and *TS/RRM2* gene silencing enhanced BxPc3 and Panc1 tumor sensitivity to gemcitabine in a higher way than did Ad-dCK::UMK or TS/RRM2 siRNA alone. This combined treatment sensitizes the resistant Panc1 tumor model, as well as the BxPc3-sensitive model to gemcitabine, indicating that our tritherapy is applicable to both resistant and sensitive tumor models. Furthermore, mice treated with TS/RRM2 siRNA alone demonstrated a nonsignificant therapeutic effect, thus indicating that the antitumor effect observed in TS/RRM2 siRNA plus gemcitabine–treated mice was actually related to gemcitabine. The *in vivo* tumor therapy study using the Panc1 orthotopic pancreatic tumor model demonstrated that tumor sensitization to gemcitabine by simultaneous treatment with Ad-dCK::UMK and TS/RRM2 siRNA resulted in a significant reduction of tumor growth. All animals had statistically significant tumor volume inhibition, with one third of animals showing complete tumor regression. The survival of mice receiving this combined therapy protocol was improved. Tumor biopsies from mice receiving simultaneous administration of gemcitabine and Ad-dCK::UMK plus TS/RRM2 siRNA presented increased apoptotic cells as determined by tumor TUNEL analysis and a low number of proliferating cells. The dramatic reduction of tumor growth may involve a bystander effect due to intercellular transfer of active and/or inactive gemcitabine through transporters. It may also involve transfer of apoptotic signals and notably the TRAIL ligand that will attach to corresponding receptors on neighboring cells. Indeed, although it is not fully understood which signals are involved in these important processes, it has been suggested that metabolites specifically generated in dying cells such as uric acid [47] or apoptotic metabolites that are activated during apoptosis could be transferred for bystander death [48]. Results were all the more interesting; as gemcitabine was administered IP after a relative low-dose schedule (15 mg/kg three times for 1 week) compared with the conventional higher used doses reported in the literature (45-380 mg/kg) [49]. Nevertheless, hepatotoxicity of the therapeutic regimens was assessed. Results demonstrated only a slight nonsignificant variation of aspartate aminotransferase, alanine aminotransferase, and bilirubin levels in the combined group compared with the gemcitabine-treated group (data not shown).

Taken together, our finding suggest for the first time that combined gemcitabine with TS/RR siRNA and dCK::UMK–based gene therapy may indeed provide a chance to treat both gemcitabine-sensitive and gemcitabine-resistant pancreatic tumors that are relatively refractory to conventional gemcitabine treatment.

Acknowledgments

The authors thank Tiraby Gerard for providing pVIVOTKSh-DU. The authors also thank Pasupathy Shanker for his critical review of the manuscript.

References

[1] Yeo TP, Hruban RH, Leach SD, Wilentz RE, Sohn TA, Kern SE, Iacobuzio-Donahue CA, Maitra A, Goggins M, Canto MI, et al. (2002). Pancreatic cancer. *Curr Probl Cancer* **26**, 176–275.

[2] Kollmannsberger C, Peters HD, and Fink U (1998). Chemotherapy in advanced pancreatic adenocarcinoma. *Cancer Treat Rev* **24**, 133–156.

[3] Burris HA, Moore MJ, Andersen J, Green MR, Rothenberg ML, Modiano MR, Cripps MC, Portenoy RK, Storniolo AM, Tarassoff P, et al. (1997). Improvements in survival and clinical benefit with gemcitabine as first-line therapy for patients with advanced pancreatic cancer: a randomized-trial. *J Clin Oncol* **15**, 2403–2413.

[4] Burris H and Storniolo AM (1997). Assessing clinical benefit in the treatment of pancreas cancer: gemcitabine compared to 5-fluorouracil. *Eur J Cancer* **33** (Suppl), 18–22.

[5] Rothenberg ML, Moore MJ, Cripps MC, Andersen JS, Portenoy RK, Burris HA III, Green MR, Tarassoff PG, Brown TD, Casper ES, et al. (1996). A phase II trial of gemcitabine in patients with 5-FU–refractory pancreas cancer. *Ann Oncol* **7**, 347–353.

[6] Abratt RP, Bezwoda WR, Falkson G, Goedhals L, Hacking D, and Rugg TA (1994). Efficacy and safety profile of gemcitabine in non–small cell lung cancer. Phase II study. *J Clin Oncol* **12**, 1535–1540.

[7] Lund B, Hansen OP, Theilade K, Hansen M, and Neijit JP (1994). Phase II study of gemcitabine (2′,2′-difluorodeoxycytidine) in previously treated ovarian cancer patients. *J Natl Cancer Inst* **86**, 1530–1533.

[8] Heinemann V (2001). Gemcitabine: progress in the treatment of pancreatic cancer. *Oncology* **60**, 8–18.

[9] Heinemann V, Schulz L, Issels RD, and Plunkett W (1995). Gemcitabine: a modulator of intracellular nucleotide and deoxynucleotide metabolism. *Semin Oncol* **22**, 11–18.

[10] Bouffard DY, Laliberte J, and Momparler RL (1993). Kinetic studies on 2′,2′-difluorodeoxycytidine (gemcitabine) with purified human deoxycytidine kinase and cytidine deaminase. *Biochem Pharmacol* **45**, 1857–1861.

[11] Plunkett W, Huang P, Xu YZ, Heinemann V, Grunewald R, and Gandhi V (1995). Gemcitabine: metabolism, mechanism of action, and self-potentiation. *Semin Oncol* **22** (Suppl), 3–10.

[12] Heinemann V, Hertel LW, Grindey GB, and Plunkett W (1988). Comparison of the cellular pharmacokinetics and toxicity of 2,2-difluorodeoxycytidine and 1-β-D-arabinofuranosylcytosine. *Cancer Res* **48**, 4024–4031.

[13] Huang P, Chubb S, Hertel LW, Grindey GB, and Plunkett W (1991). Action of 2′,2′-difluorodeoxycytidine on DNA synthesis. *Cancer Res* **51**, 6110–6117.

[14] Ruiz van Haperen VW, Veerman G, Vermorken JB, and Peters GJ (1993). 2′,2′-Difluoro-deoxycytidine (gemcitabine) incorporation into RNA and DNA of tumour cell lines. *Biochem Pharmacol* **46**, 762–766.

[15] Bergman AM, Pinedo HM, and Peters GJ (2002). Determinants of resistance to 2′,2′-difluorocytidine (gemcitabine). *Drug Resist Updat* **5**, 19–33.

[16] Beausejour CM, Gagnon J, Primeau M, and Momparler RL (2002). Cytotoxic activity of 2′,2′-difluorodeoxycytidine, 5-aza-2′-deoxycytidine and cytosine arabinoside in cells transduced with deoxycytidine kinase gene. *Biochem Biophys Res Commun* **293**, 1478–1484.

[17] Galmarini CM, Clarke ML, Jordheim L, Santos CL, Cros E, Mackey JR, and Dumontet C (2004). Resistance to gemcitabine in a human follicular lymphoma cell line is due to partial deletion of the deoxycytidine kinase gene. *BMC Pharmacol* **4**, 8.

[18] Bergman AM, Giaccone G, van Moorsel CJ, Mauritz R, Noordhuis P, Pinedo HM, and Peters GJ (2000). Cross-resistance in the 2′,2′-difluorodeoxycytidine (gemcitabine)–resistant human ovarian cancer cell line AG6000 to standard and investigational drugs. *Eur J Cancer* **36**, 1974–1983.

[19] Manome Y, Wen PY, Dong Y, Tanaka T, Mitchell BS, Kufe DW, and Fine HA (1996). Viral vector transduction of the human deoxycytidine kinase cDNA sensitizes glioma cells to the cytotoxic effects of cytosine arabinoside *in vitro* and *in vivo*. *Nat Med* **2**, 567–573.

[20] Van der Wilt CL, Kroep JR, Bergman AM, Loves WJ, Alvarez E, Talianidis I, Eriksson S, van Groeningen CJ, Pinedo HM, and Peters GJ (2000). The role of deoxycytidine kinase in gemcitabine cytotoxicity. *Adv Exp Med Biol* **486**, 287–290.

[21] Van Rompay AR, Johansson M, and Karlsson A (2000). Phosphorylation of nucleosides and nucleoside analogs by mammalian nucleoside monophosphate kinases. *Pharmacol Ther* **87**, 189–198.

[22] Galmarini CM, Mackey JR, and Dumontet C (2001). Nucleoside analogues: mechanisms of drug resistance and reversal strategies. *Leukemia* **15**, 875–890.

[23] Galmarini CM, Mackey JR, and Dumontet C (2002). Nucleoside analogues and nucleobases in cancer treatment. *Lancet Oncol* **3**, 415–424.

[24] Vernejoul F, Laurent Ghénassia L, Souque A, Lulka H, Drocourt D, Cordelier P, Pradayrol L, Pyronnet S, Buscail L, and Tiraby G (2006). Gene therapy based on gemcitabine chemosensitization suppresses pancreatic tumor growth. *Mol Ther* **14**, 758–767.

[25] Goan YG, Zhou B, Hu E, Mi S, and Yen Y (1999). Overexpression of ribonucleotide reductase as a mechanism of resistance to 2,2-difluorodeoxycytidine in the human KB cancer cell line. *Cancer Res* **59**, 4204–4207.

[26] Eriksson S and Martin DW Jr (1981). Ribonucleotide reductase in cultured mouse lymphoma cells. Cell cycle–dependent variation in the activity of subunit protein M2. *J Biol Chem* **256**, 9436–9440.

[27] Duxbury MS, Ito H, Zinner MJ, Ashley SW, and Whang EE (2004). RNA interference targeting the M2 subunit of ribonucleotide reductase enhances pancreatic adenocarcinoma chemosensitivity to gemcitabine. *Oncogene* **23**, 1539–1548.

[28] Graham FL and Prevec L (1991). Manipulation of adenovirus vectors. In Murray EJ (ed.), *Methods in Molecular Biology. Gene Transfer and Expression Protocols,* vol. 7, Clifton, NJ: The Humana Press, Inc., 109–128.

[29] Peng HH, Wu S, Davis JJ, Wang L, Roth JA, Marini FC III, and Fang B (2006). A rapid and efficient method for purification of recombinant adenovirus with RGD-modified fibers. *Anal Biochem* **354**, 140–147.

[30] Mackey JR, Mani RS, Selner M, Mowles D, Young JD, Belt JA, Crawford CR, and Cass CE (1998). Functional nucleoside transporters are required for gemcitabine influx and manifestation of toxicity in cancer cell lines. *Cancer Res* **58**, 4349–4357.

[31] Arlt A, Vorndamm J, Breitenbroich M, Fölsch UR, Kalthoff H, Schmidt WE, and Schäfer H (2001). Inhibition of NF-kappaB sensitizes human pancreatic carcinoma cells to apoptosis induced by etoposide (VP16) or doxorubicin. *Oncogene* **20**, 859–868.

[32] Nakano Y, Tanno S, Koizumi K, Nishikawa T, Nakamura K, Minoguchi M, Izawa T, Mizukami Y, Okumura T, and Kohgo Y (2007). Gemcitabine chemoresistance and molecular markers associated with gemcitabine transport and metabolism in human pancreatic cancer cells. *Br J Cancer* **96**, 457–463.

[33] Duxbury MS, Ito H, Zinner MJ, Ashley SW, and Whang EE (2004). Inhibition of SRC tyrosine kinase impairs inherent and acquired gemcitabine resistance in human pancreatic adenocarcinoma cells. *Clin Cancer Res* **10**, 2205–2207.

[34] Giroux V, Malicet C, Barthet M, Gironella M, Archange C, Dagorn JC, Vasseur S, and Iovanna JL (2006). p8 is a new target of gemcitabine in pancreatic cancer cells. *Clin Cancer Res* **12**, 235–241.

[35] Bergman AM, Eijk PP, Ruiz van Haperen VW, Smid K, Veerman G, Hubeek I, van den Ijssel P, Ylstra B, and Peters GJ (2005). *In vivo* induction of resistance to gemcitabine results in increased expression of ribonucleotide reductase subunit M1 as the major determinant. *Cancer Res* **65**, 9510–9516.

[36] Van der wilt CL, Pinedo HM, Smid K, and Peters GJ (1992). Elevation of thymidylate synthase following 5-fluorouracil treatment is prevented by the addition of leucovorin in murine colon tumors. *Cancer Res* **52**, 4922–4928.

[37] Csapo Z, Sasvari-Szekely M, Spasokoukotskaja T, Talianidis I, Eriksson S, and Staub M (2001). Activation of deoxycytidine kinase by inhibition of DNA synthesis in human lymphocytes. *Biochem Pharmacol* **61**, 191–197.

[38] Shrikhande SV, Kleeff J, Kayed H, Keleg S, Reiser C, Giese T, Büchler MW, Esposito I, and Friess H (2006). Silencing of X-linked inhibitor of apoptosis (XIAP) decreases gemcitabine resistance of pancreatic cancer cells. *Anticancer Res* **26**, 3265–3273.

[39] Denlinger CE, Rundall BK, Keller MD, and Jones DR (2004). Proteasome inhibition sensitizes non–small-cell lung cancer to gemcitabine-induced apoptosis. *Ann Thorac Surg* **78**, 1207–1214.

[40] Pace E, Melis M, Siena L, Bucchieri F, Vignola AM, Profita M, Gjomarkaj M, and Bonsignore G (2000). Effects of gemcitabine on cell proliferation and apoptosis in non small cell lung cancer (NSCLC) cell lines. *Cancer Chemother Pharmacol* **46**, 467–476.

[41] Ferreira CG, Tolis C, Span SW, Peters GJ, van Lopik T, Kummer AJ, Pinedo HM, and Giaccone G (2000). Drug-induced apoptosis in lung cancer cells is not mediated by the Fas/FasL (CD95/APO1) signaling pathway. *Clin Cancer Res* **6**, 203–212.

[42] Wack S, Rejiba S, Parmentier C, Aprahamian M, and Hajri A (2008). Telomerase transcriptional targeting of inducible *Bax/TRAIL* gene therapy improves gemcitabine treatment of pancreatic cancer. *Mol Ther* **16**, 252–260.

[43] Lin T, Zhang L, Davis J, Gu J, Nishizaki M, Ji L, Roth JA, Xiong M, and Fang B (2003). Combination of *TRAIL* gene therapy and chemotherapy enhances

antitumor and antimetastasis effects in chemosensitive and chemoresistant breast cancers. *Mol Ther* **8**, 441–448.

[44] Arlt A and Schäfer H (2002). NFkappaB-dependent chemoresistance in solid tumors. *Int J Clin Pharm Ther* **40**, 336–347.

[45] Wang W, Abbruzzese JL, Evans DB, and Chiao PJ (1999). Overexpression of urokinase-type plasminogen activator in pancreatic adenocarcinoma is regulated by constitutively activated RelA. *Oncogene* **18**, 4554–4563.

[46] Dong QG, Sclabas GM, Fujioka S, Schmidt C, Peng B, Wu T, Tsao MS, Evans DB, Abbruzzese JL, McDonnell TJ, et al. (2002). The function of multiple IkappaB : NF-kappaB complexes in the resistance of cancer cells to Taxol-induced apoptosis. *Oncogene* **21**, 6510–6519.

[47] Mattson MP, Goodman Y, Luo H, Fu W, and Furukawa K (1997). Activation of NF-kappaB protects hippocampal neurons against oxidative stress–induced apoptosis: evidence for induction of manganese superoxide dismutase and suppression of peroxynitrite production and protein tyrosine nitration. *J Neurosci Res* **49**, 681–697.

[48] Krysko DV, Leybaert L, Vandenabeele P, and D'Herde K (2005). Gap junctions and the propagation of cell survival and cell death signals. *Apoptosis* **10**, 459–469.

[49] Pratesi G, Petrangolini G, Tortoreto M, Addis A, Belluco S, Rossini A, Selleri S, Rumio C, Menard S, and Balsari A (2005). Therapeutic synergism of gemcitabine and CpG-oligodeoxynucleotides in an orthotopic human pancreatic carcinoma xenograft. *Cancer Res* **65**, 6388–6393.